Assessment of process-induced microcracks in 3D woven composites using meso-scale model simulations

Nikolay V Timoshchuk*, Kent D Kasper and Harun H Bayraktar

Albany Engineered Composites Inc, 216 Airport Drive, Rochester, NH 03867, USA

* nikolay.timoshchuk@albint.com

Abstract. One of the advantages of 3D woven composites is the ability to create unique fiber architectures in which tows can be individually arranged to optimize performance to meet specific structural requirements. This flexibility may lead to a design with unintended mismatch of thermal properties in areas of the composite, creating the potential for manufacturing issues such as process-induced microcracking. This paper presents results of a case study in which various architectures were analyzed, including some that led to intra-tow microcracks in the molded composite and others that did not. The objective was to develop an approach using meso-scale finite element modeling at the unit cell level to evaluate the propensity of these architectures to microcrack. Analysis results showed that the transverse principal stresses which developed in tow elements during cooling from cure to room temperature were significantly different in the various architectures. Comparison to the micro-computed tomography scans of the molded composites established strong correlation between regions with microcracks and areas of high predicted transverse principal stresses in the simulations. This study suggests that meso-scale finite element modeling of 3D woven architectures can be used in the design cycle to reduce or eliminate microcracking in the finished composite parts.

1. Introduction

Superior fatigue resistance and damage tolerance of 3D woven composites over traditional 2D laminates [1] made this class of composites an obvious choice for a number of applications, particularly in the aerospace arena. Some examples where 3D composites provide a significant advantage include: integrally woven T- and Pi-joints, cruciforms, outer guide vanes, and various 3D woven fittings. The most widespread applications are the fan blades and fan cases used in the LEAP turbofan engines, which currently power the Boeing 737 MAX and Airbus A320neo series aircraft [2].

An ability to create unique fiber assemblies (i.e. architectures) where tows can be individually arranged for optimal performance coupled with a possibility to tailor thickness by adding or dropping layers offers great flexibility in designing 3D woven preforms. Such flexibility, however, heightens the risk of creating a design with potentially large mismatch in thermal properties within the composite, which can lead to process-induced microcracks in the finished part. The cost associated with evaluating multiple part designs for the propensity to microcrack by means of experimental testing can be high and the turnover rates low. Therefore, a validated simulation approach which ties the meso- and macro-scale modelling of 3D woven composites and takes into account preform level design features such as layer drops could provide a great practical advantage in evaluation of architecture designs prior to manufacture.

IOP Conf. Series: Materials Science and Engineering **406** (2018) 012053 doi:10.1088/1757-899X/406/1/012053

Understanding process-induced microcracks in 3D woven composites was attempted by researchers in the past. Tsukrov et al [3] utilized micro-scale numerical modeling of a representative as-woven textile geometry to predict microcracking of carbon fiber/epoxy composites during resin curing. They relied on the parabolic failure stress criterion to study two typical 3D woven architectures, orthogonal and ply-to-ply, to assess their propensity to microcrack by comparing parabolic stresses developed within resin pockets. They found that the orthogonal architecture exhibited higher parabolic stresses, both in cumulative sense across the entire unit cell as well as locally, thus having a higher potential to produce microcracking during curing. They were able to correlate the regions of high parabolic stresses with the locations of microcracks as observed in the scans obtained by micro-computed tomography (μCT).

The microcracks presented in this paper appear to be different in nature compared to those analyzed by Tsukrov et al, and found not only within resin pockets but primarily through the tows as shown in micrograph in figure 1(a) below.

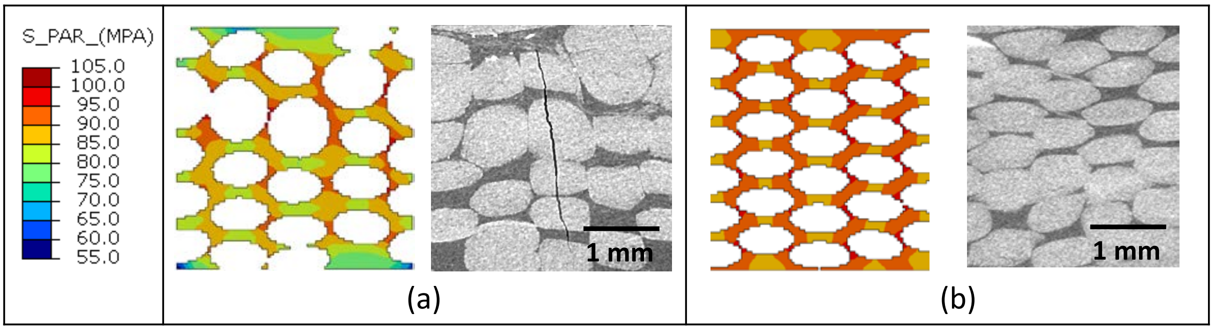

Figure 1. Two 3D woven architectures showing (a) microcracks and a lower level of the predicted parabolic stress, and (b) no microcracks and a higher level of the predicted parabolic stress.

By applying the parabolic stress failure criterion, no correlation was established between the levels of parabolic stresses as predicted by meso-scale FEA modeling and intra-tow microcracks as detected in μCT scans. In fact, the parabolic stresses were found to be higher for the architecture that did not exhibit microcracking as shown in figure 1(b). This suggests that for the type of intra-tow microcracks discussed in this paper a different approach is necessary in order to predict this type of failure in 3D woven composites.

2. VERVE™ property predictions

Albany Engineered Composites Inc. uses a proprietary method to assess the performance of 3D woven composites using meso-scale modeling of realistic 3D woven architectures on the unit cell level. This method relies on conducting Virtual Experiments on Representative Volume Element (VERVE™) to extract the equivalent stiffness matrix [4], which makes it possible to predict effective elastic constants of an RVE. VERVE™ can also be used to extract the effective thermal and electrical constants. With the application of periodic boundary conditions (PBCs), the performance of a unit cell can represent the performance of an entire part or coupon which makes VERVE™ a powerful virtual surrogate technique to study property changes due to process and material variations [5]. Additionally, models generated by VERVE™ allow one to visualize the spatial variations in stress/strain developed within a unit cell, a level of detail often necessary to identify regions and/or certain features of an architecture responsible for stress concentrations and/or failure.

An example of a meso-scale finite element unit cell model of a 3D woven composite visualized by Abaqus/CAE software (Version 6.14-1, Dassault Systèmes Simulia Corp., Providence, RI) is shown in figure 2. This example plots the stresses developed along the longitudinal directions of a tow, after applying load in the global X (warp) direction. Elements representing the surrounding resin were removed for clarity.

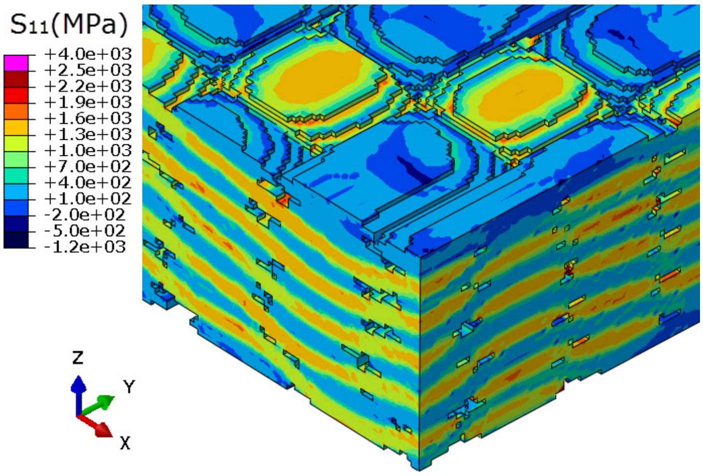

Figure 2. VERVE™ model of a 3D woven architecture.

By conducting a series of virtual tests, all nine independent material constants of a unit cell representing an orthotropic material can be determined. These effective properties can be used as input to the finite element analysis of a part on the macro-scale level, where tows and resin are no longer modeled exclusively due to computational time and machine capacity limitation considerations. This method of meso-scale modeling can also be applied to applications that have a more specific set of load and boundary conditions, as it was used in this study to understand the effects of residual stresses on microcracking in 3D woven composites.

2.1. Selected Architectures

Four 3D woven fiber architectures considered in this paper are presented in figure 3. They have attributes of either (or both, in case of A3) ply-to-ply or orthogonal topologies, which are two common types in 3D woven composite designs. Topology is a general term that is used to describe the weave pattern without specifying any of the parameters associated with it such as number of layers, warp and weft column spacing, tow types, etc. Architecture is considered to be a specific case of a topology with all those parameters defined.

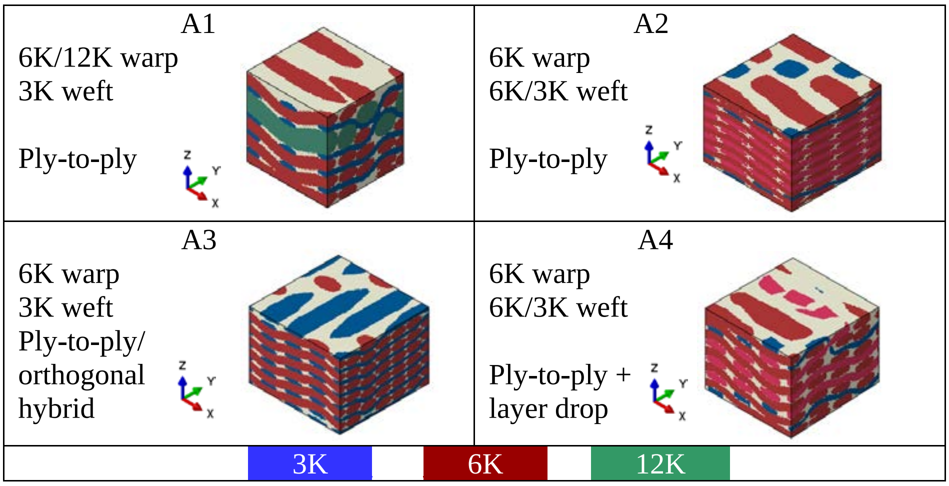

Figure 3. 3D woven architectures created using meso-scale model simulations.

A1 and A2 were two ply-to-ply architectures in which all fibers provide layer-to-layer interlocking (i.e. first layer interlocks with second, second with third, etc. until all layers are interlocked).

Architecture A1 also used two different tow sizes, 6K and 3K, in the X (warp) direction which was not the case in any other architecture where the warp tow size was kept constant. Architecture A3 had attributes of both ply-to-ply and orthogonal topologies. In orthogonal topologies, there are two sets of fibers: stuffers, which are essentially straight yarns, and weavers which dive between top and bottom surfaces interlocking all layers. A3 had a combination of stuffers (i.e. orthogonal feature) as well as layer-to-layer interlocking (i.e. ply-to-ply feature). A4 was a special case of a ply-to-ply architecture with a layer drop in the Y (weft) direction, a design feature most commonly thought of as a preform-level detail. The layer drop was implemented by exiting a yarn immediately under the surface yarn.

All architectures were modeled using the unit cell approach. In 3D woven composites, a unit cell is considered to be a building block for the whole textile, such that the preform can be created by assembling the unit cells in warp and weft directions, sometimes in the through-thickness direction as well. A unit cell can vary in size depending on how many warp and weft columns are necessary to define the architecture but generally can be as little as 2 by 2 and as large as 10 by 10 columns.

2.2. Material properties and material orientations

All 3D composites considered in this paper utilized Toho's HTA carbon fiber tows in 12K, 6K, and 3K sizes, depending on the architecture. Physical coupons that were used for validation were injected by resin transfer molding (RTM) using Tactix 123 resin system. A homogenization technique based on composite cylinder assemblage (CCA) and upper/lower bounds on the elastic constants as given by Hashin [6] was used to obtain tow properties with a tow packing factor in the range of 0.7-0.8. The transversely isotropic tow properties were mapped onto the tow elements with the axis of material symmetry lined up with the longitudinal direction determined from known positions of centroid points for each tow. The matrix was treated as an isotropic material with the temperature-independent Young's modulus, Poisson's ratio and coefficient of thermal expansion.

2.3. Boundary conditions and loadcases

VERVE™ employs periodic boundary conditions as a way to study the behavior of an entire part or a coupon by considering just a single representative volume element or a unit cell of that structure. PBCs exist in a form of equations relating the displacement on one part of the boundary to those on another [7]. Full periodic boundary conditions (i.e. periodicity in X, Y and Z directions) were applied to all architectures considered in this study, except for architecture A4 which, due to a layer drop, maintained periodicity in X direction only.

All property predictions were calculated based on the linear perturbation analysis completed within Abaqus/CAE. Simulations intended to extract the elastic constants involved six steps necessary to construct the equivalent stiffness matrix: three axial and three shear load cases in each of the three primary directions and on three primary planes, respectively. Thermal expansion coefficients were determined from the change in RVE dimensions due to a uniform temperature drop of 1ºC.

2.4. Effective properties

Effective elastic and thermal properties for each of four architectures as predicted by meso-scale model simulations are summarized in table 1. A significant difference in fiber volumes used in these four cases as well as in values of material constants suggests a different internal state of stress that these composites would likely to experience during the curing cycle.

IOP Conf. Series: Materials Science and Engineering **406** (2018) 012053 doi:10.1088/1757-899X/406/1/012053

Table 1. Effective properties of architectures A1 – A4.

	A1 (*Vf=0.56*)	A2 (*Vf=0.58*)	A3 (*Vf=0.64*)	A4 (*Vf=0.58*)
E_1 (GPa)	62.8	61.4	88.9	50.9
E_2 (GPa)	13.7	42.7	32.9	25.1
E_3 (GPa)	8.4	9.8	10.7	9.2
G_{12} (GPa)	3.1	3.4	4.2	3.3
G_{13} (GPa)	4.4	3.2	4.3	3.9
G_{23} (GPa)	2.9	3.2	3.7	3.6
ν_{12}	0.19	0.13	0.16	0.24
ν_{13}	0.81	0.51	0.55	0.59
ν_{23}	0.48	0.53	0.5	0.55
α_1 ($\mu\varepsilon/^oC$)	-1.46	1.66	0.489	0.353
α_2 ($\mu\varepsilon/^oC$)	17	3.38	5.3	5.15
α_2 ($\mu\varepsilon/^oC$)	37.2	42	35.6	38.6

These values were used as the material properties for the 3D woven core in the macro-scale analysis as discussed in Section 3.

3. Cure-induced microcracking in 3D composite core

3D woven preforms were molded with 2D cover plies attached to top and bottom surfaces (figure 4), which possess different elastic and thermal properties compared to those of the 3D composite core. The constraint due to the addition of cover plies yielded a different state of residual stress experienced by the core from a uniform temperature drop, compared to an unconstrained case. This paper does not discuss in detail the cooldown analysis on the macroscopic level, however, the strain output from these models was used to define the boundary conditions in meso-scale level simulations as described in Section 3.1.

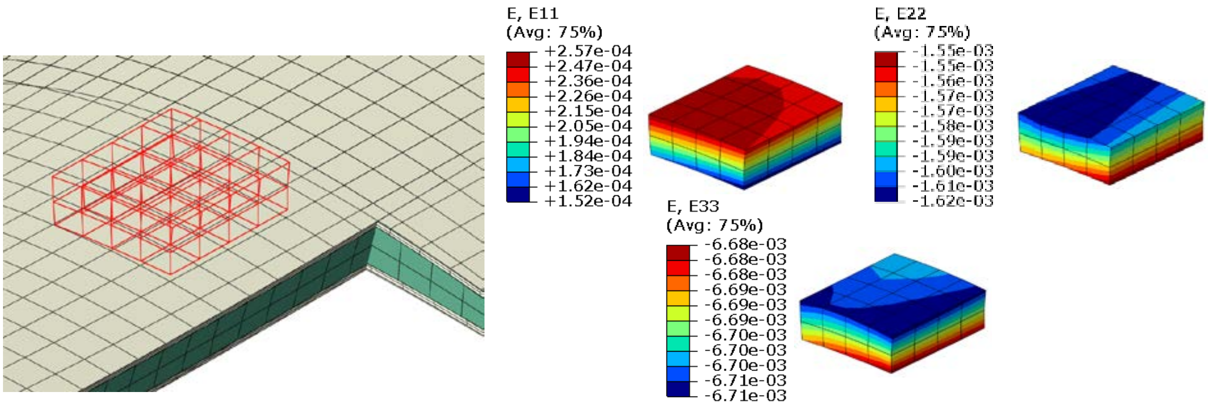

(a) (b)

Figure 4. Partial view of the macro-scale model showing (a) 2D cover plies on both sides of the 3D woven core with the area of interest corresponding to an approximate area where most microcracks were observed in molded parts, and (b) the amount of strain experienced by the core in that region.

The comparison charts that demonstrate the difference in strains as predicted in constrained versus unconstrained cases are shown in figure 5 for (a) direction-2 (i.e. weft direction), and for (b) direction-3 (i.e. through-thickness direction). Strains in direction-1 (i.e. warp direction) for both meso- and macro-scale models were found to be negligible and thus were not shown.

(a) (b)

Figure 5. Comparison of microstrain in (a) direction-2 (weft direction), and (b) through-thickness direction between constrained and unconstrained cases.

In most cases the difference was less than 10%, particularly for microstrain in the through-thickness direction. The biggest difference was observed in $\mu\varepsilon_{22}$ for architecture A1 which suggests that in order to predict a more accurate state of stress in a 3D woven core it is necessary to take into account the contribution of 2D cover plies that effect the overall response. Failure to do so could lead to wrong conclusions as it relates to microcracking in those cases. To account for the contribution of 2D cover plies in meso-scale thermal analysis, the microstrains $\mu\varepsilon_{22}$ and $\mu\varepsilon_{33}$ were included as direct boundary conditions.

3.1. Meso-scale thermal analysis

The meso-scale unit cell models for all four architectures presented in Section 2 that were used to obtain the effective elastic and thermal constants were modified to apply an uniform temperature drop from cure to room temperature. Two major adjustments that were made included: (1) changing the temperature drop from 1ºC to 165ºC, and (2) prescribing a fixed amount of displacement in directions 2 and 3, to match the results of the macro-scale analysis for each architecture.

3.2. Transverse principal stresses

The type of microcracks discussed in this paper appear to occur not only in resin pockets, but more so through the tows of 3D woven composites, as was shown in figure 1. Presumably, the stresses acting in the transverse plane of a transversely-isotropic tow were significant enough to split a tow, forming a microcrack. The maximum and minimum values attained by the normal stress in the plane of isotropy could provide an insight into this type of failure. The meso-scale models of four architectures considered in this paper were post-processed to calculate the principal normal stresses (i.e. transverse principal stresses) according to the following expression:

$$\sigma_{TPS1}, \sigma_{TPS2} = \frac{\sigma_{22}+\sigma_{33}}{2} \pm \left(\left(\frac{\sigma_{22}-\sigma_{33}}{2}\right)^2 + \tau_{23}^2\right)^{1/2} \quad (1)$$

where 2 and 3 are tow directions in the plane of transverse isotropy.

3.3. Validation by micro-computed tomography scans

The hypothesis that transverse principal stresses can be used to evaluate the propensity of an architecture to exhibit the intra-tow microcracks due to cure-induced stresses was validated by comparing the results of the meso-scale model simulations with the micro-computed tomography scans as shown in figure 6. The µCT images correspond to the same warp and weft columns for which transverse principal stresses are shown. There appears to be a strong correlation between architectures with high TPS1 and whether or not those architectures exhibited microcracking. Architecture A1 and A4 both have considerably higher TPS1 compared to A2 and A3, reaching in excess of 115-120 MPa. The locations of microcracks tend to correlate with areas of stress concentration.

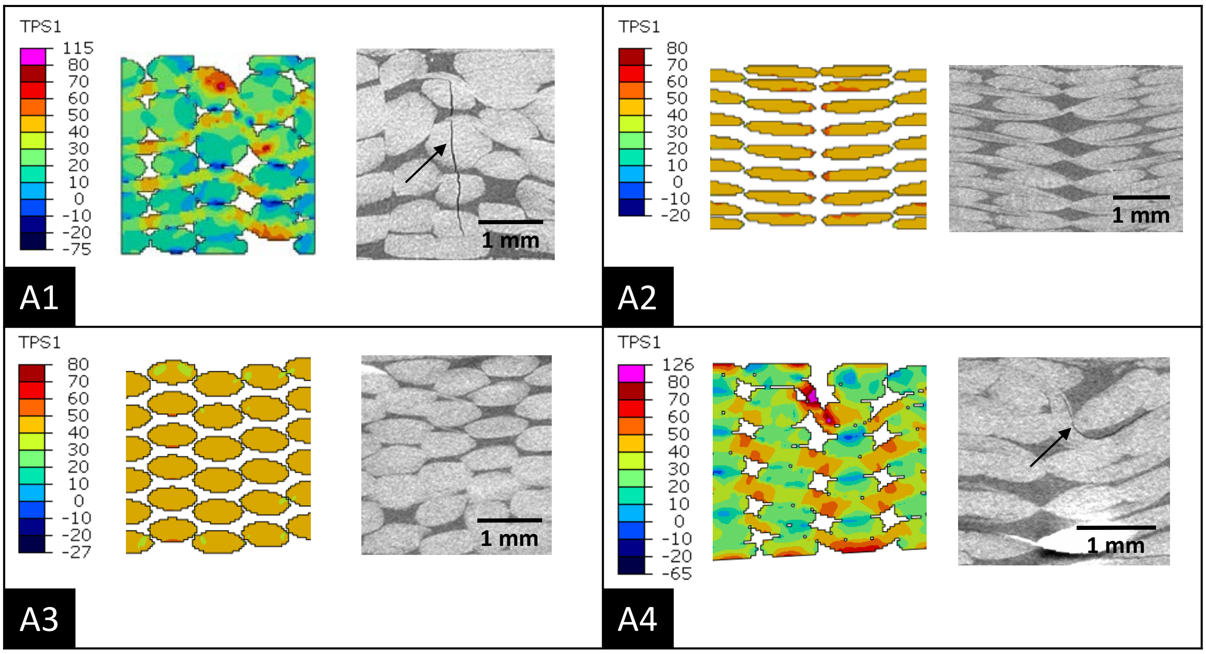

Figure 6. Comparison of areas with high transverse principle stresses and locations of microcracks.

One common feature found in architectures A1 and A4, both of which exhibited microcracking, is an abrupt change in the direction of the top surface yarn relative to other yarns, violating the through-thickness design symmetry and likely contributing to a mismatch in composite properties locally. In case of A1, the symmetry was violated even more by insertion of 12K in place of 6K tows in the second layer from the top surface. These features may not always lead to microcracking in 3D woven composites but can be avoided during the architecture design to reduce the risk of composite failure.

The magnitudes of the second component of the transverse principal stress TPS2 were found to be considerably smaller and, therefore, were not shown. Presumably, the positive (tensile) stresses were largely responsible for creating the microcracks as it appears the tows were pulled apart (TPS1) as opposed to being compressed (TPS2). The strong correlation between the areas of high transverse principal stresses as predicted by meso-scale modeling and the locations of microcracks observed by µCT demonstrates the merits of the approach presented.

4. Conclusions

A mismatch in thermal properties in areas of 3D woven composites, which can vary greatly depending on the architecture selection, can lead to process-induced microcracking in the finished product. A robust finite element simulation approach can add value by providing an ability to evaluate designs for their propensity to microcrack under residual stresses without a need to manufacture physical parts. The meso-scale modeling effort presented in this paper shows that:

- Relying on a parabolic stress failure criterion alone may not fully capture the likelihood of microcracking in the composite part.
- Evaluating transverse principal stresses within tow elements can identify whether intra-tow microcracking is likely to occur, and can be especially useful when comparing alternate architecture designs.

- Incorporating the effects of the macroscopic assembly of 2D and 3D materials can be a critical contributor to evaluating the cure-induced stresses in the composite part, and the coupling of macro- and meso-scale analyses can further separate performance of different architectures.
- Abrupt changes in tow direction and variations in tow size symmetry through the cross section, while perhaps unavoidable in the design of a monolithic preform, can have a non-negligible effect on process induced microcracking.

References

[1] Tong L, Mouritz A P and Bannister M K 2002 *3D Fibre Reinforced Polymer Composites* (Oxford: Elsevier Science)
[2] Dambrine B, Mahieu J-N, Goering J and Ouellette 2008 Development of 3D woven resin transfer molded fanblades *Proc. 9th Int. Conf. Textile Composites TEXCOMP9 Recent Advances in Textile Composites* ed S Advani and J Gillespie Jr (Lancaster, PA: DEStech Publications) pp 19-24
[3] Tsukrov I, Bayraktar H, Giovinazzo M, Goering J, Gross T, Fruscello M and Martinsson L 2011 Finite element modeling to predict cure-induced microcracking in three-dimensional woven composites *Int. J. Fracture* **172** pp 209-16
[4] Ehrlich D, Bayraktar H and Kelley J 2015 Using Different Homogenization Techniques for Different Stages of Product Development for 3D Woven Composites *Proc. 12th Int. Conf. Textile Composites TEXCOMP12* (Raleigh, NC: North Carolina State University)
[5] Cowles B, Backman D, Dutton R 2012 Verification and Validation of ICME Methods and Models for Aerospace Applications *Integrating Materials and Manufacturing Innovation* **1**
[6] Hashin Z 1972 *Theory of Fiber-Reinforced Materials* (Washington DC: NASA). Hashin Z 1979 Analysis of Properties of Fiber Composites with Anisotropic Constituents *J Appl. Mech. Transcations ASME* **46** pp 543-50
[7] Li S 2001 General unit cells for micromechanical analyses of unidirectional composites *Compos. Part A Appl. Sci. Manuf.* **32** pp 815-26